Nonlinear Response for Time Dependent External Fields:

Shear Flow and Color Conductivity

Janka Petravic and Denis J. Evans

Research School of Chemistry, Australian National University, Canberra, Australian Capital Territory 0200, Australia 2

ABSTRACT

We present a generalisation of the nonlinear response theory for autonomous systems which can be applied to classical many-body systems in large time-dependent external fields. Our formalism represents the first practical application of response theory to such problems, and provides a method of evaluating averages of phase functions which is more efficient than direct computer simulation. Our expressions for the nonlinear time dependent response are tested against nonequilibrium molecular dynamics computer simulation of two simple nonautonomous systems. The relation of our results to known special cases (time-dependent linear response and time independent nonlinear response) is discussed.

KEY WORDS: dynamic response; nonlinear systems; external flows; many-body problems; nonequilibrium flow; molecular dynamics method; simulation

1. INTRODUCTION

When the external field perturbing a classical *N*-particle system is sufficiently weak, the linear response theory [1,2] yields the expressions for the transport coefficients in terms of the equilibrium properties of the system. This provides a complete treatment of response to any constant or time-dependent external fields for which the linear approximation holds.

For constant fields, the general nonlinear response can be found using either of the two equivalent methods, Kawasaki response formula [3] or the transient time-correlation function (TTCF) approach [4]. The derivations of both theories rely on the fact that the equations of motion of constituent particles do not depend on time explicitly.

There have been attempts to develop a formalism for treatment of nonlinear response to time-dependent fields [5], which use the time-ordered exponentials for the definition of propagators. However, due to commutivity constraints, the resulting expressions were too complex to be used in comparisons with laboratory, or even computer experiments.

Recently [6,7], we described an entirely new approach to the treatment of nonlinear non-autonomous systems. Our approach is based on the definition of an extended phase space in which the system becomes autonomous.

The algorithm corresponding to this extended phase space TTCF formalism is tested using computer simulation of two very simple systems. The first consists of two coloured disks interacting with a colour sensitive, time dependent, external field, and we compare the response of field induced changes in the hydrostatic pressure to that predicted by our theory. The second system consists of two disks subjected to steady shear. The standard nonequilibrium molecular dynamics algorithm for steady shear flow (Sllod) employs Lees–Edwards [8] periodic boundary conditions. It is not widely known that these boundary conditions make the system non–autonomous, and the "steady state" shear stress is in fact time periodic. The changes in the hydrostatic pressure in the first

example and the time-dependence of the shear stress in the second example are both entirely nonlinear effects, and provide an emphatic validation of the theory.

Somewhat surprisingly our extended TTCF approach enables the calculation of these time dependent effects with greater computational efficiency than direct observation. This improved efficiency is apparent even in the presence of very strong applied fields.

2. THEORY

We consider a general isokinetic N -particle system subject to a time dependent external field which is introduced at t = 0. The equations of motion of such a system are

$$\dot{\mathbf{q}}_{i} = \frac{\mathbf{p}_{i}}{m} + \mathbf{C}_{i}()F_{e}(t)$$

$$\dot{\mathbf{p}}_{i} = \mathbf{F}_{i} + \mathbf{D}_{i}()F_{e}(t) - \mathbf{p}_{i},$$
(1)

where the Gaussian thermostat multiplier , given by

$$= \frac{\frac{\mathbf{F}_{i}}{m} \mathbf{p}_{i}}{\frac{\mathbf{p}_{i}^{2}}{m} + \frac{\mathbf{p}_{i}}{m} \mathbf{p}_{i}} + \frac{\mathbf{p}_{i}}{m} F_{e}, \qquad (2)$$

constrains the peculiar kinetic energy $K = \frac{1}{i} \mathbf{p}_i^2 / 2m$ to a constant of motion. The state of the system can be represented by a point in the phase space—spanned by $(\mathbf{q}_i, \mathbf{p}_i; i = 1,...N)$. We assume that the external field is periodic in time, so that $F_e(t + T_e) = F_e(t)$.

For t = 0, the external field is zero and the system is assumed to be at equilibrium. The time-independent equilibrium phase space probability distribution of the isokinetic system is

$$f_0(\) = \frac{\exp[-\ U(\)]\ (K(\) - K_0)}{d\ \exp[-\ U(\)]\ (K(\) - K_0)},\tag{3}$$

where U is the potential energy of the system, $K_0 = dN/2$ is the kinetic energy, $= 1/k_BT$ where T is the temperature, k_B the Boltzmann constant and d is the Cartesian dimensionality of the system.

After the time dependent external field starts acting upon the system (at t=0), the phase space probability distribution changes from $f_0(\cdot)$ towards a periodic long time non-equilibrium distribution, $f_0(\cdot) = f_0(\cdot, t) + T_e(\cdot)$.

Therefore the explicit time-dependence affects a non-autonomous system in two different ways. Firstly, the system approaches the long time distribution through a sequence of transient states, which is analogous to the case of autonomous systems. Secondly, the long time distribution itself is time dependent.

This complex picture [5], can be simplified by incorporating a new variable,

$$(t) = + t, (4)$$

which is directly proportional to time, into the equations of motion (1),

$$\dot{\mathbf{q}}_{i} = \frac{\mathbf{p}_{i}}{m} + \mathbf{C}_{i}()F_{e}()$$

$$\dot{\mathbf{p}}_{i} = \mathbf{F}_{i} + \mathbf{D}_{i}()F_{e}() - \mathbf{p}_{i}$$

$$\vdots = . \tag{5}$$

The new variable is the generalisation of the "phase angle" of the trigonometric functions. The *linear* time dependence of this additional phase space coordinate is essential for the development of the extended TTCF algorithm, because it enables one to reach exactly the prescribed values of after a given number of timesteps. The state of the system can now be represented by a point in *extended* phase space, $=(\ ,\)=(\mathbf{q}_i,\mathbf{p}_i,\ ;\ i=1,...,N).$ Because of the periodicity of the external field F_e , it is sufficient to consider values of in the range $[0,\ T_e].$

For systems governed by (5), the equilibrium extended phase space distribution $f_0(\)$ is uniform in $\ ,\ f_0(\)d\ = \left(f_0(\)/\ T_e\right)d\ d\ .$

For systems where the long time macroscopic averages are not sensitively dependent on the initial phase = (,), the long time distribution f () will be time-independent, but dependent on $\,$. This is analogous to the approach to a unique steady state in autonomous systems. The only time dependence comes from the change of f_0 () to f () when the external field F_e () is applied. Clearly this lack of sensitivity to the

initial phase will eventually break down if the external field is sufficiently strong. We do not consider such systems here.

Let us consider a phase variable $B(\cdot)$ which is a function of \cdot , and which by definition does not explicitly depend on time, or therefore on the additional phase space . Although $B(\)$ is solely a function of $\$, we can see from the equations of motion, (5), that the phase that the system evolves to at time t, namely (t), is a function of the initial *extended* phase, = (,). Thus it is more revealing to write, B(t) = B(t) (t; ,)). In order to know the value of a phase function at time t, in addition to the elapsed time, we need to specify the initial phase vector and the initial phase of the external field. angle

The average over extended phase space of B, taken at time t, is

$$\langle B(t) \rangle = d \ f(\ ,t)B(\) = d \ f(\ ,0)B(\ (t;\))$$

$$= d \ f_0(\)B(\ (t;\ ,\)) = d \ d \ \frac{f_0(\)}{T_0}B(\ (t;\ ,\)), \tag{6}$$

in the Schrödinger and Heisenberg pictures, respectively. As the equilibrium distribution $f_0($) is known and given by (3), it is simpler to use the Heisenberg picture. Using the definition of the dissipative flux J, [9],

$$\mathbf{C}_{i}(\) \mathbf{F}_{i} - \mathbf{D}_{i}(\) \frac{\mathbf{p}_{i}}{m} J(\),$$

and the adiabatic incompressibility of phase space condition [9] (AI), one can show that since,

$$\frac{d\langle B(t)\rangle}{dt} = - \quad d \quad B((t; ,))F_e()J()f_0(),$$

integrating with respect to time yields
$$\langle B(t) \rangle = \langle B(0) \rangle - \int_{0}^{t} ds \langle B((s; (0), (0))) F_{e}((0)) J((0)) \rangle. \tag{7}$$

The expression (7) describes the evolution of the extended phase space average of the phase variable after the external field is applied. The average over the extended phase space means an average over all possible initial combinations of positions, momenta and the additional phase-space coordinate . If B were taken to be the dissipative flux then $\langle J(t) \rangle = 0$, by symmetry. The fact that the extended average of the dissipative flux vanishes illustrates that the average taken in (7) is not what we are most interested in. We shall now consider averages taken over the standard phase space for a particular value of $= P_{p}$ at time t.

The expression corresponding to the Heisenberg picture in (6) is

$$\langle B(\ (t);\ (t) = \ _{p} \rangle = \langle B(\ (t)\ (\ (t) - \ _{p}) \rangle$$

$$= d \ f_{0} (\)B(\ (t;\ ,\ = \ _{p} - \ t)) \ (\ (t) - \ _{p}) \ .$$

Using the same procedure as above, we find that the averages taken over the standard phase space for a particular value of = p at time t are given by

$$\langle B(\ (t;\ (t) = P)) \rangle = \langle B(\ (0;\ (0) = P)) \rangle$$

$$- \int_{0}^{t} ds F_{e}(\ P - s) \langle B(\ (s;\ (s) = P)) J(\ (0;\ (0) = P - s)) \rangle.$$
 (8)

The average value $\langle B(t); (t) = P_p \rangle$ in (8) means the average over all values of the phase , at the time t, for a particular chosen constant value, $_{p}$, of the phase angle (t); (t) = $_{p}$. If all possible values of $_{p}$ from the interval $[0, T_{e}]$ are at time t, substituted into (8), the dependence of $\langle B(t); (t) = P_p \rangle$ on P_p at the time t can be found. It should be pointed out that this dependence cannot be obtained by direct calculations from a set of trajectories starting from the **single** initial value of (0). Such a set could only give the value of $\langle B(t); (t) = t \rangle$ at the time t, $\langle B((t+t); (t) = (t+t) \rangle$ at the time t+t, etc. It should also be observed that in the integrals on both sides of (8) (s) is a constant equal to $_{P}$. However, as the time s changes, trajectories which contribute to the correlation function at some particular value of s change. For different times s they start at different initial values of $_0 = _P - _S$. Therefore, in order to find the evolution of $\langle B(t); (t) = P_p \rangle$ for the chosen value of $(t) = P_p$, we need to know the behaviour of trajectories with **all** possible initial (0) at all previous times.

The expression (8) is the general expression for the nonlinear response to a timedependent external field. For time-independent fields, there is no dependence in the distribution function, and all extended phases that differ only in the extended phase space coordinate become identical, so that (8) reduces to the TTCF formula for autonomous systems [1]. The linear time dependent response formula [1], applicable in the low amplitude and high frequency limit, is obtained from (8) if the equilibrium correlation function is substituted for the transient correlation in the integrand of (8).

3. TEST SYSTEM: COLOUR CONDUCTIVITY

This formalism is illustrated by the example of nonequilibrium molecular dynamics simulation of a system of two disks with periodic boundary conditions, subject to a time-dependent colour field [10].

The interaction \mathbf{F}_i between disks is characterised by the WCA (Weeks-Chandler-Anderson) potential [11]. In this work the effective diameter of the disks, , the depth of the potential well of the corresponding Lennard-Jones potential, , and the particle mass m, are all set to unity.

The disks differ by colour labels, $c_i = (-1)^i$, i = 1,2, which determine the interaction of each disk with the external colour field $F_c(t)$ acting in the x direction. We assume a sinusoidal time dependence of the colour field for t > 0, $F_c(t) = F_0 \sin(_0 + t)$.

The additional coordinate is defined from (4) so that the equations of motion for t > 0 in *extended* phase space $= (\mathbf{q}_i, \mathbf{p}_i,); i = 1,2$ are

$$\dot{\mathbf{q}}_i = \frac{\mathbf{p}_i}{m},$$

$$\dot{\mathbf{p}}_{i} = \mathbf{F}_{i} + \mathbf{i}c_{i}F_{0}\sin - \mathbf{p}_{i},$$

$$\cdot = , \qquad (9)$$

with the thermostatting term given by (3).

In this system, the dissipative flux is given by $J = c_i \dot{x}_i$, and the response of the hydrostatic pressure, P,

$$P = \frac{1}{2} (P_{xx} + P_{yy}) = \frac{1}{2V} \left\langle \sum_{i=1}^{N} \frac{p_{xi}^2 + p_{yi}^2}{m} + x_i F_{xi} + y_i F_{yi} \right\rangle, \tag{10}$$

to a sinusoidal colour field was monitored as a function of the angle t. The response was calculated from (8) with B replaced by P.

The simulations were done at the density =N/V=0.396850 and at the temperature T=1.0, using the fourth-order Runge-Kutta method of integration of the equations of motion (9) with a timestep of t=0.002.

The simulations were carried out for 2x50000 initial phases from the isokinetic equilibrium ensemble, for each of the 100 initial values of (0), and for a time 0 < t < 5. From each starting phase $= (\mathbf{q}_i, \mathbf{p}_i)$, an additional starting point was generated using the time-reversal mapping $\mathbf{M}^{\mathrm{T}}(\) = (\mathbf{q}_i, -\mathbf{p}_i)$, in order to improve the statistics and to reduce the systematic error. This additional starting point ensures that the average initial current is identically zero.

The equilibrium correlation function under the time integral in (8), $\langle P(t)J_x(0)\rangle$, vanishes at all times, and therefore in the linear approximation the pressure is just equal to its equilibrium value. However, for strong fields the pressure oscillates with twice the frequency of the external field (since it is even under \mathbf{M}^T). The pressure shift is a strictly nonlinear effect and therefore provides a powerful test of our theory. In Fig. 1 are shown the results obtained by the direct simulation and the time-dependent TTCF method. Since the effect is very small, the direct simulation data are very noisy and therefore there is still some disagreement at early times. At late times, the agreement between the two sets of calculations is excellent. This agreement is all the more remarkable because of the complex shape of the response curves and the fact that these responses are entirely nonlinear. The chance of accidental agreement, particularly in Fig. 1(b), must be negligible.

In Fig. 1(b) we see the response for (t) = 0, and for $(t) = \frac{72.3}{2}$. By symmetry the response in each of these pairs should be identical. The disparity gives a reasonable estimate of the statistical uncertainty in the TTCF and the direct response curves. Although the direct and the extended TTCF curves are computed from the same number of simulation timesteps, the extended TTCF curves always have a smaller

variance. This is somewhat surprising given that the field amplitude is so large (TTCF methods will always be more efficient than direct methods at sufficiently small fields.). We believe that this improvement in efficiency is related to the fact that in Eq. (8) the response at a given time and specified phase angle is computed from an ensemble average of trajectory responses which span the initial phase angle distribution. This cross phase averaging results in superior efficiency.

4. TEST SYSTEM: STEADY SHEAR FLOW

The non-equilibrium steady states of the planar Couette-Taylor flow have been successfully simulated using the Sllod [9] algorithm with the Lees-Edwards boundary conditions [8]. The Sllod equations of motion for the two dimensional two-body system are

$$\dot{\mathbf{q}}_{i} = \mathbf{p}_{i} / m + \mathbf{i} \quad y_{i} ,$$

$$\dot{\mathbf{p}}_{i} = \mathbf{F}_{i} - \mathbf{i} \quad p_{yi} - \mathbf{p}_{i} ,$$
(11)

where \mathbf{p}_i is the momentum of the i-th particle and \mathbf{q}_i its position in the periodic cell. The parameter is the shear rate (= u_x/y , where \mathbf{u} is the streaming velocity) and is the Gaussian thermostat which ensures the conservation of the peculiar kinetic energy at all times. \mathbf{F}_i is the interaction between the particle i and particle j within its minimum image cell [9]. It is given by WCA interaction potential [11].

The Lees-Edwards periodic boundary conditions define the motion of the neighbouring periodic cells to be consistent with the linear streaming velocity profile in the equations of motion (11). The motion of the cell images is such that their individual origins move with an x-velocity proportional to the y coordinate of the particular cell origin. If L is the sidelength of the square periodic cell, the relative displacement d_xL of the origin of its neighbour on top will depend on time as

$$d_{x}(t) = \text{mod}(d_{x}(0) + t, 1). \tag{12}$$

This causes the symmetry of the lattice to change periodically in time with the period of 1/. Note that $d_x(t)$ is the strain of the lattice defined by Lees-Edwards periodic boundary conditions. Since the interaction of particles is determined by the minimum image

convention, the periodic moving boundary conditions (12) affect the interaction between particles periodically in time. Therefore in the Sllod equations (11) it is more proper to write $\mathbf{F}_i(t)$ instead of \mathbf{F}_i because the particle interactions explicitly depend on the instantaneous symmetry of the lattice and therefore on time.

We are usually interested in the phase space average of some phase function B some time after application of the external shearing field. It can be expected that even in the long time limit t the steady state of this two disk system will not exist, but that $\langle B \rangle$ will be time-periodic because of the time dependence implicit in the boundary conditions. The generalised TTCF theory derived in the Section 2 can be modified to correctly describe this kind of time-dependence, if the additional extended phase space coordinate—is defined to be d_x [7]. We have only to keep in mind that in this case the d_x dependence of the equations of motion (11) is present even in equilibrium when—0, because we can consider stationary periodic lattices of different symmetries, characterised by different constant values of d_x . The equilibrium phase space distribution function $f_0(\cdot)$ will generally depend on d_x , therefore it is more precise to write $f_0(\cdot, d_x)$.

While the oscillations in $\langle B \rangle$ present in small systems subjected to constant shear are just an artefact of the boundary conditions, the evolution of the extended phase space average of $B(\)$, as in (7), can be related to the values of this phase function in real systems. The extended phase space average at long times is the same as the average over one period of oscillation.

The response of the shear stress,

$$P_{xy} = \frac{1}{V} \left\langle \sum_{i=1,2} \frac{P_{xi}P_{yi}}{m} + \frac{1}{2} \sum_{\substack{j=1,2\\j \ i}} (x_{ij}F_{yij} + y_{ij}F_{xij}) \right\rangle,$$

has been monitored as a function of the shift of neighbour cells d_x and time t. It has been calculated from the expression corresponding to (8),

$$\langle P_{xy}((t;d_x(t)=D)) \rangle = \langle P_{xy}((0;d_x(0)=D)) \rangle$$

$$- V \int_0^t ds \langle P_{xy}((s;d_x(s)=D)) P_{xy}((0;d_x(0)=D-s)) \rangle.$$
(13)

The simulation results for a 2 disk system at the reduced strain rate $*=(m/)^{1/2}=1$ are shown in Fig.2. The simulations were done at the reduced density $={}^2=0.396850$ and at the reduced temperature $T=k_BT/=1.0$, using the fourth-order Runge-Kutta method of integration of the equations of motion (1) with a timestep of t=0.005. The interval [0,1] of possible values of d_x has been divided into 50 subintervals of width $d_x=0.02$, and the timestep of time integration in (13) is therefore ds=0.02. From each starting phase $=(\mathbf{q}_i,\mathbf{p}_i;d_x)$ of the isokinetic equilibrium ensemble, three additional starting points were generated using the time-reversal mapping \mathbf{M}^T , the y-reflection mapping \mathbf{M}^Y , and the Kawasaki mapping \mathbf{M}^K [9],

$$\mathbf{M}^{\mathrm{T}}() = (\mathbf{q}_{i}, -\mathbf{p}_{i}; -d_{x}),$$

$$\mathbf{M}^{\mathrm{Y}}() = (x, -y, z, p_{x}, -p_{y}, p_{z}; d_{x}),$$

$$\mathbf{M}^{\mathrm{K}}() = (x, -y, z, -p_{x}, p_{y}, -p_{z}; -d_{x}),$$

in order to improve the statistics and to reduce systematic error. These additional starting phase points ensure that the average initial shear stress is identically zero. Since the objective of this simulation has been to test whether the direct calculations and our theory (13) coincide, we used a large number of initial trajectories, 4x20000 for each of the 50 values of $d_x(0)$.

When the shear stress correlation function in (13) is integrated over the same time t for many different lattice configurations $d_x = D$, the dependence of P_{xy} on d_x at time t is obtained. This dependence first changes its form, and after a long time (in this case the time of 5/ was found to be sufficient), when the system reaches its steady state in the extended phase space, the form of the d_x dependence remains constant in time. The evolution of the shear stress response as a function of d_x , evaluated by direct simulation and using the generalised TTCF formula (13), is shown in Fig.2a. After the the system has been subjected to shear for a short time (t=0.5 in Fig.2a) the variations of P_{xy} with the change of d_x are small. Later the amplitude of oscillations increases until a final state pattern is established.

Fig.2b shows the approach to the steady state of $P_{xy}((t; d_x(t)=D))$ for four values of D. In Fig. 2c the phase space average of P_{xy} has been evaluated from the trajectories starting from the same equilibrium lattice, with $d_x(0)=0$ and was followed over five periods of the lattice symmetry change. In all these results, there is an excellent correspondence between direct and TTCF calculations, but there is less noise present in the TTCF results. Noise reduction is a feature typical of all TTCF methods [6,7].

5. CONCLUSION

The generalisation of the TTCF formalism to nonautonomous systems has been developed by extending the phase space to include an additional coordinate, , which is linearly dependent on time and which is incorporated into the equations of motion. The *linear* time dependence of this additional phase space coordinate is essential for the development of the extended TTCF algorithm, because it enables one to reach exactly the prescribed values of after a given number of timesteps. The equations of motion in the *extended* phase space become autonomous, and the response is governed by the time evolution of the probability distribution f() of the extended phase space as a whole.

The simulation results for the test case of the response of the colour current to a sinusoidal colour field for a periodic two disk system, shows excellent agreement between the extended TTCF approach and the direct simulation. The comparison of results for the intrinsically nonlinear field induced pressure shift is even more impressive. Even at comparatively large fields, the extended TTCF approach yields results with superior computational efficiency to direct simulation.

We have pointed out that for 'steady' shear flow under Lees-Edwards shearing periodic boundary conditions, the equations of motion are in fact non-autonomous. The effects of these non-autonomous terms decrease extremely rapidly with increasing system size, N. We expect however, that for systems with long ranged potentials this will not be so. For finite N, in the nonlinear regime conventional (autonomous) response theory for steady shear flow is incorrect. Our generalisation of time dependent nonlinear response

theory successfully describes steady Lees-Edwards shear flow. We have tested this theory against nonequilibrium computer simulation and found impressive agreement between theory and experiment. This agreement is all the more impressive because of the irregular and complex shapes of the response curves.

A bonus from our theory is that when it is used to compute the response one obtains estimates of the response which are more accurate than those obtained by directly averaging the observed response. This enhanced efficiency is thought to result from the non deterministic sampling of the phase space coordinate which depends linearly on time. This sampling results in an efficient exploration of the extended phase space.

One disadvantage of this theory is that it can only be applied to periodic fields. Another disadvantage is that the results are relevant only to periodic fields of the same frequency and waveform. For example, we cannot use the results of the present simulations for sinusoidal fields to predict the response of the same system to strong square waves fields, or indeed, to sinusoidal fields of different frequencies of amplitudes.

REFERENCES

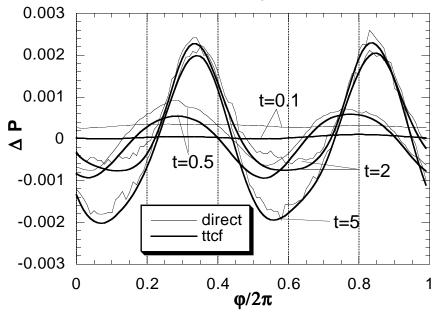
- [1] M. S. Green, J. Chem. Phys. 22, 398 (1954);R. Kubo, J. Phys. Soc. Jpn. 12, 570 (1957).
- R. Zwanzig, Ann. Rev. Phys. Chem., 16, 67(1965);
 R. Zwanzig, Lectures on Theoretical Physics, Vol III, p135, Wiley (Interscience), New York (1961).
- [3] T. Yamada and K. Kawasaki, Prog. Theor. Phys. **38**, 1031 (1967).
- [4] W. M. Vischer, Phys. Rev. A 10, 2461 (1974);
 J. W. Dufty and M. J. Lindenfeld, J.Stat.Phys. 20, 259 (1979);
 E. G. D. Cohen, Physica (Amsterdam) 118A, 17 (1983);
 G. P. Morriss and D. J. Evans, Mol. Phys. 54, 629 (1985);
 G. P. Morriss and D. J. Evans, Phys. Rev. A 35, 792 (1987).
- [5] D. J. Evans and G. P. Morriss, Mol. Phys. 64, 521 (1988);B. L. Holian and D. J. Evans, J. Chem. Phys. 83, 3560 (1985).
- [6] J. Petravic and D. J. Evans, Phys. Rev. Letts. 78, 1199 (1997)J. Petravic and D. J. Evans, Phys. Rev. E (accepted)
- [7] J. Petravic and D. J. Evans, Phys. Rev. E (submitted)
- [8] A. W. Lees and S. F. Edwards, J. Phys. **C5**, 1921 (1975)
- [9] D. J. Evans and G. P. Morriss, *Statistical Mechanics of Nonequilibrium Liquids*, (Academic Press, New York, 1990).
- [10] D. J. Evans, W. G. Hoover, B. H. Failor, B. Moran and A. J. C. Ladd, Phys. Rev. A 28, 1016 (1983).
- [11] J. D. Weeks, D. Chandler and H.C. Andersen, J. Chem. Phys. **54**, 5237 (1971).

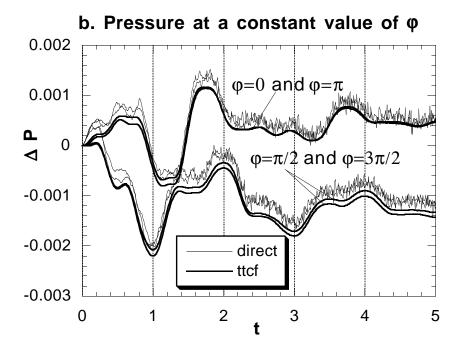
FIGURE CAPTIONS

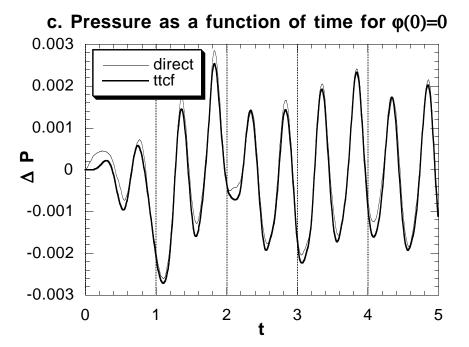
FIGURE 1. The direct simulation and TTCF results for the pressure in the periodic colour field. Both the direct simulation and the TTCF results show that the pressure oscillates with twice the frequency of the colour field. The amplitude of the pressure oscillations changes in time from zero to the final value. (a) Pressure as a function of at different times. (b) Pressure at a constant value of . (c) Pressure as a function of time for (0)=0.

FIGURE 2. (a) The change of the d_x dependence of the shear stress of a two disc system in time, evaluated using direct simulation and the generalised TTCF method. (b) The shear stress of a of a two disc system with *=1 has different steady state values for different lattice configurations d_x . The approach to the steady state is calculated for four different configurations using direct simulation and the generalised TTCF method. The two methods show excellent correspondence of results, but there is less noise present in the TTCF results. (c) Direct simulation and TTCF results for the time evolution of the shear stress of a two disc system with *=1, starting from the lattice configuration characterised by $d_x(0)$ =0. The two sets of results coincide in these graphs.

a. Pressure as a function of ϕ at different times







a. Shear stress as a function of d_x at different times

